A Multicarrier Primer

John M. Cioffi
Amati Communications Corporation and Stanford University
408-257-1717 or 415-723-2150

Abstract

This tutorial describes fundamentals of multicarrier modulation, and how it is analyzed, for channels with intersymbol interference and additive Gaussian noise. This document was prepared specifically for Bellcore personnel to facilitate their analysis of multicarrier modulation methods for Asymmetric Digital Subscriber Line (ADSL) services.

The presented analysis permits the determination of the best data rate using multicarrier on a given channel with a specified margin. We also show how to compute the margin for a given fixed data rate. The multicarrier analysis uses single-carrier concepts extensively so that someone already familiar with single carrier can more quickly analyze multicarrier.

Contents

1 Introduction to Multicarrier

This section describes multicarrier and introduces notation to be used in the analysis of later sections.

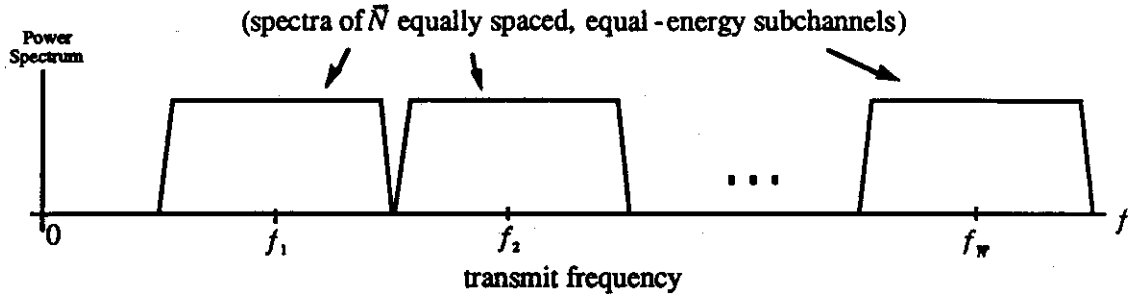

Figure 1: Transmit power spectrum of a multicarrier signal.

1.1 Frequency-Division Fundamentals of Multicarrier

Fundamentally, multicarrier modulation superimposes several carrier-modulated waveforms to represent an input bit stream. The transmitted power spectrum of a multicarrier waveform is illustrated in Figure 1. The multicarrier transmit signal is the sum of $\bar{N}$ independent sub-signals, each of equal bandwidth and with center frequency f_i, $i = 1, ..., \bar{N}$. Each of these sub-signals, or **subchannels** as they are often called, can be considered to be a Quadrature Amplitude Modulated (QAM) signal. In multicarrier modulation, as opposed to conventional frequency-division multiplexing, the number of bits of input data that are allocated to different subchannels can be different. The parsing of bits to subchannels is coordinated by the multicarrier modulator to maximize performance. In maximizing performance, subchannels that will encounter less channel attenuation and/or more noise will carry more bits of information.

Bandlimited communication channels, in particular subscriber loops, exhibit variation in gain and phase with frequency. On such channels, multicarrier modulation has been long known to be optimum when $\bar{N}$ is large [1]. Nevertheless, most early attempts at the implementation of multicarrier modulation failed because of the difficulty in maintaining the equal spacing of the subchannels shown in Figure 1. More recent attempts at multicarrier modulation have been successful for two reasons: (1) the advent of digital signal processors that can accurately synthesize the sum of modulated waveforms and (2) the introduction of the Fast Fourier Transform (FFT) that can be used to efficiently compute this sum for large $\bar{N}$. With the use of digital signal processing and the FFT, multicarrier modulation schemes have recently been used very successfully in high-speed modems (Telebit, IMC, NEC) and in all digital audio broadcast systems, proposed (North America) and standardized (Europe's Eureka 147). It also appears that the upcoming direct broadcast (satellite and/or terestrial) digital television services may now also use multicarrier modulation to eliminate transmission problems with multipath fading. In all these systems, the exceptionally high performance of multicarrier is achieved because of the digital implementation with FFT's. In all cases, $\bar{N}$ is a power of two so that efficient versions of the FFT can be used and the size of this FFT is $N = 2\bar{N}$.

The size of $\bar{N}$ required to approximate optimum performance depends roughly on how rapidly the transfer function of a bandlimited channel varies with frequency. In the analysis of this short report, we will always assume that $\bar{N}$ is chosen sufficiently large to approximate optimum performance. In the appendix, we show a preferred method for the subscriber-loop application that ensures that $\bar{N} = 256$ is sufficient to achieve optimum performance levels. To analyze the performance of a multicarrier modulation scheme on a particular channel, one need only know the value of $\bar{N}$ chosen (and not necessarily how that $\bar{N}$ was chosen), which is why we defer further discussion of the choice of $\bar{N}$ to the appendix.

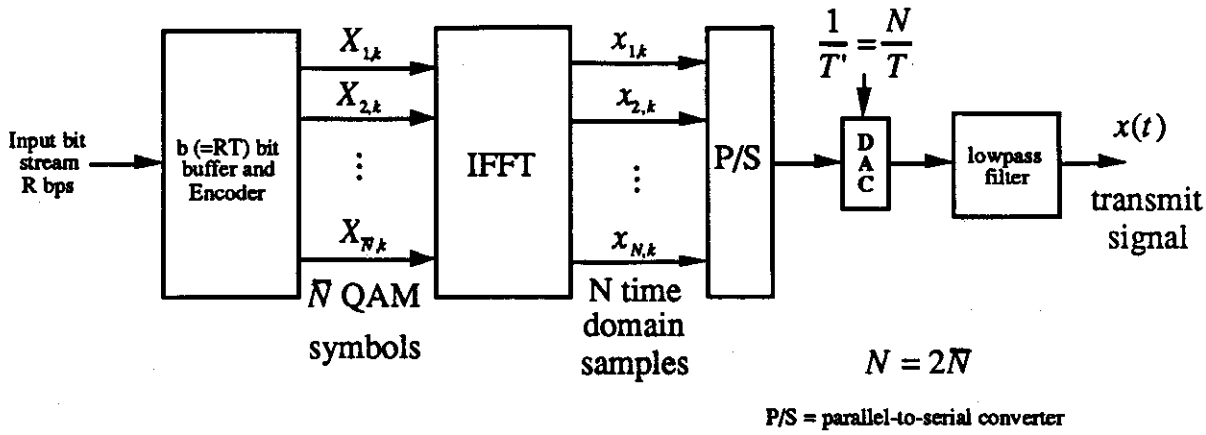

Figure 2: Illustration of DMT transmitter for large $\bar{N}$.

1.2 Discrete Multitone Modulation

Discrete Multitone (DMT) is a common form of multicarrier modulation. It was introduced by Peled and Ruiz of IBM in 1980 [2] to take advantage of digital signal processors and the FFT. It was later refined to a very high-performance form by Ruiz, Cioffi, and Kasturia [3], [4]. That latter form is used in the most recent multicarrier voiceband modems, and also in one of the digital audio broadcast proposals [5]. DMT has also been investigated for HDSL and ADSL in [6] and [7], respectively.

The basic DMT system is illustrated for large N in Figure 2 [1]. An input bit stream of **data rate** R bits/second (bps) is buffered into blocks of $b = RT$ bits, where T is called the **symbol period** (in seconds) and $1/T$ is called the **symbol rate**. The transmitted signal over the symbol period is called the **symbol**. Of these b bits, b_i $(i = 1, ...\bar{N})$ are intended for use in the i^{th} subchannel and

$$b = \sum_{i=1}^{\bar{N}} b_i \quad . \tag{1}$$

These b_i bits for each of the $\bar{N}$ subchannels are translated in the DMT encoder into a complex **subsymbol**, X_i, with amplitude $|X_i|$ and phase $\angle X_i$. The quantity X_i can be viewed as the amplitude of the i^{th} QAM signal in multicarrier modulation. There are 2^{b_i} possible values for this subsymbol. Successive blocks of b bits are processed in an identical manner. We use a second subscript of k on $X_{i,k}$ to denote the i^{th} subsymbol in the k^{th} transmitted symbol.

The mean-square value of X_i is called the **subsymbol energy**, $\mathcal{E}_i$. The **subsymbol power** is given by $P_i = \mathcal{E}_i/T$. The $N = 2\bar{N}$-point IFFT (see appendix) combines the $\bar{N}$ subsymbols into a set of N real-valued time-domain **samples**, $x_{n,k}$, $n = 0, ..., N-1$, as is also shown in Figure 2. The set of N successive time-domain samples is the k^{th} symbol. These N samples in a symbol are successively applied (after conversion to serial format) to a digital-to-analog converter (DAC), which samples at rate $1/T' = N/T$, the **sampling rate** of the DMT modulator. The output of the DAC is the continuous-time modulated signal $x(t)$. Any lowpass filtering at the DAC output is presumed to be absorbed into the channel response in this tutorial. Note, $T = NT'$.

The IFFT is an example of an orthogonal transformation and preserves the energy of the input

[1] In practice, the implementation is slightly more involved than shown in Figure 2 (see the appendix) but the more involved implementation just strictly ensures that the analysis that we will present is accurate for any $\bar{N}$.

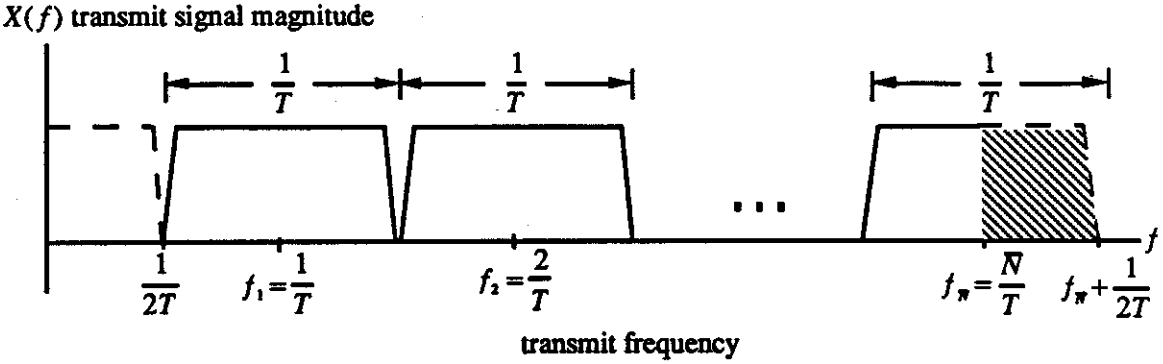

Figure 3: DMT transmit power spectrum.

frequency-domain symbol. That is,

$$\sum_{i=1}^{\bar{N}} |X_{i,k}|^2 = \sum_{n=1}^{N} x_{n,k}^2 \tag{2}$$

and thus the transmit power is

$$P = \frac{\mathcal{E}}{T} = \frac{\sum_{i=1}^{\bar{N}} \mathcal{E}_i}{T} = \sum_{i=1}^{\bar{N}} P_i \quad . \tag{3}$$

In DMT, Figure 1 is slightly altered to Figure 3. The f_i in DMT are fixed at $f_i = i/T$, $i = 1, ..., \bar{N}$. No transmit energy can occur above the frequency $1/(2T') = f_{\bar{N}}$ in DMT. Instead, what happens is that the frequency band from $f_{\bar{N}}$ to $f_{\bar{N}} + 1/(2T)$ is replaced by the vacant frequency band from 0 to $1/(2T)$, as shown in Figure 3. This can be viewed as transmitting the real part of the N^{th} symbol baseband $(0, 1/2T)$ and the imaginary part as the lower side band part of a waveform modulated at $1/2T'$. Nevertheless, we think of these two one-dimensional signals as inphase and quadrature components of a single two-dimensional QAM signal at $f_{\bar{N}} = 1/(2T')$.

1.3 The Channel and Its Effect

Figure 4 illustrates a channel with impulse response $h(t)$ and additive (Gaussian) noise $u(t)$. We call the channel output $y(t)$. We investigate the use of multicarrier modulation on such an intersymbol-inteference (ISI) channel.

When $\bar{N}$ is large, the continuous transfer function of the channel response $H(f)$ can be approximated by the discrete curve illustrated by rectangles in Figure 4. Each of the rectangles is a band of frequencies $1/T$ Hz wide. The value of the transfer function at each center frequency, $H(f_i)$, is abbreviated as H_i. The f_i in Figure 4 are the DMT center frequencies, f_i, $i = 1, ..., \bar{N}$. H_i has a magnitude $|H_i|$ and a phase $\angle H_i$. On a single subscriber loop, the magnitude of H_i often spans several orders of magnitude as the index varies. The variance per dimension of the sampled noise is denoted σ^2.

When $\bar{N}$ is sufficiently large, then the rectangles are very narrow in Figure 4, and it is mathematically correct to write

$$Y_{i,k} = H_i X_{i,k} + U_{i,k} \tag{4}$$

where $Y_{i,k}$ $i = 1, ..., \bar{N}$ are the complex outputs of the N-point FFT in Figure 5 (and $U_{i,k}$, $i = 1, ..., \bar{N}$

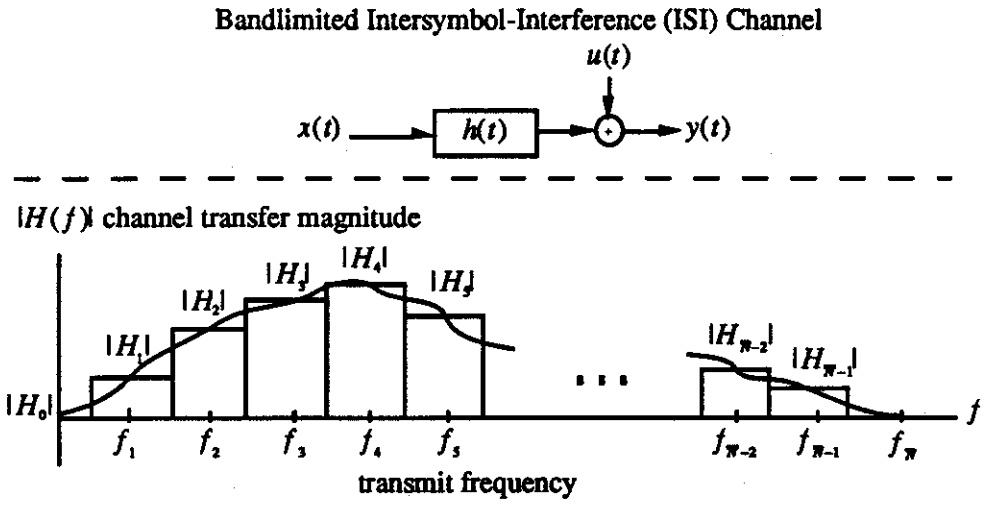

Figure 4: Channel and multichannel decomposition of channel response.

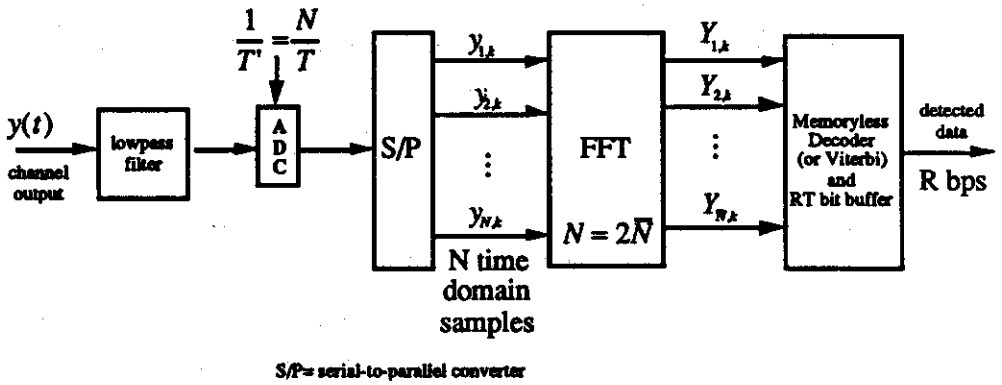

Figure 5: Receiver for DMT.

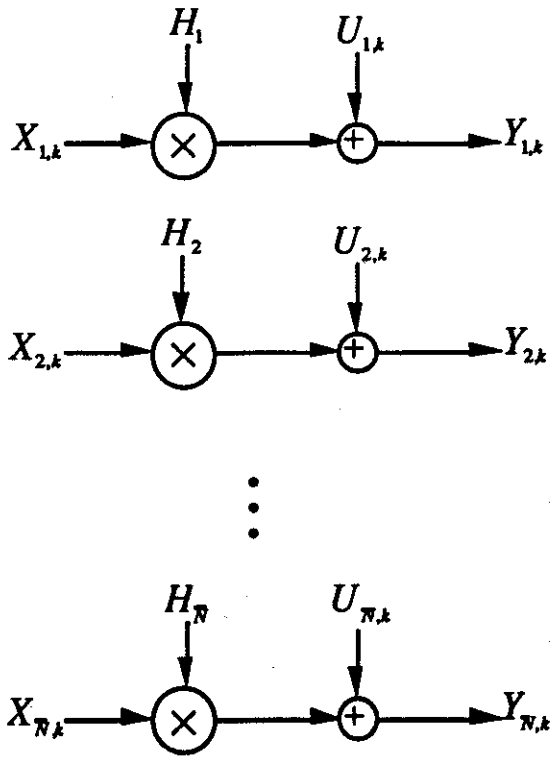

Figure 6: Set of parallel independent channels that is equivalent to the original channel when multicarrier modulation is used.

are similarly defined for the noise). That is, the $\bar{N}$ output samples of the receiver FFT correspond to $\bar{N}$ independent subchannels, i.e., with no interference between them, as is illustrated in Figure 6. When $\bar{N}$ is large, the noise components $U_{i,k}$ can be shown to be independent when $u(t)$ is Gaussian even if the noise is not white (that is, not flat in power spectrum). We assume symbol (frame) synchronization, as well as sample-clock synchronization, between the transmitter and receiver.

We note that then, because the subchannels are independent, they can be individually decoded using a memoryless detector for each. This set of memoryless detectors is the optimum maximum-likelihood detector for the transmitted signal.[2] Maximum-likelihood detection is then achieved in DMT with no equalization nor any use of sequence detection. (The price paid for DMT's optimum detection is then the IFFT/FFT, which, however, is often implemented at a small fraction of the cost of digital filtering or sequence detection for comparable situations.)

1.4 Example

As an example, consider the magnitude of the transfer function of the loop channel shown in Figure 7. This loop corresponds to the channel polynomial

$$H(D) = \sum_n h_n D^n = \frac{.1(1-D)(1+D)}{(1-.9D)(1-.6D)} = \frac{.1(1-D^2)}{1-1.5D+.54D^2} \quad , \tag{5}$$

at a sampling rate of $1/T'$=1.0 MHz. While $N = 8$ ($\bar{N} = 4$) is too small of an FFT size for the independent-subchannels assumption to hold, we will assume that the subchannels are independent anyway for the illustrative purposes of this example (an example with a larger number of subchannels

[2]In the case where trellis coding is used, the maximum likelihood detector then becomes the detector for the applied trellis code.

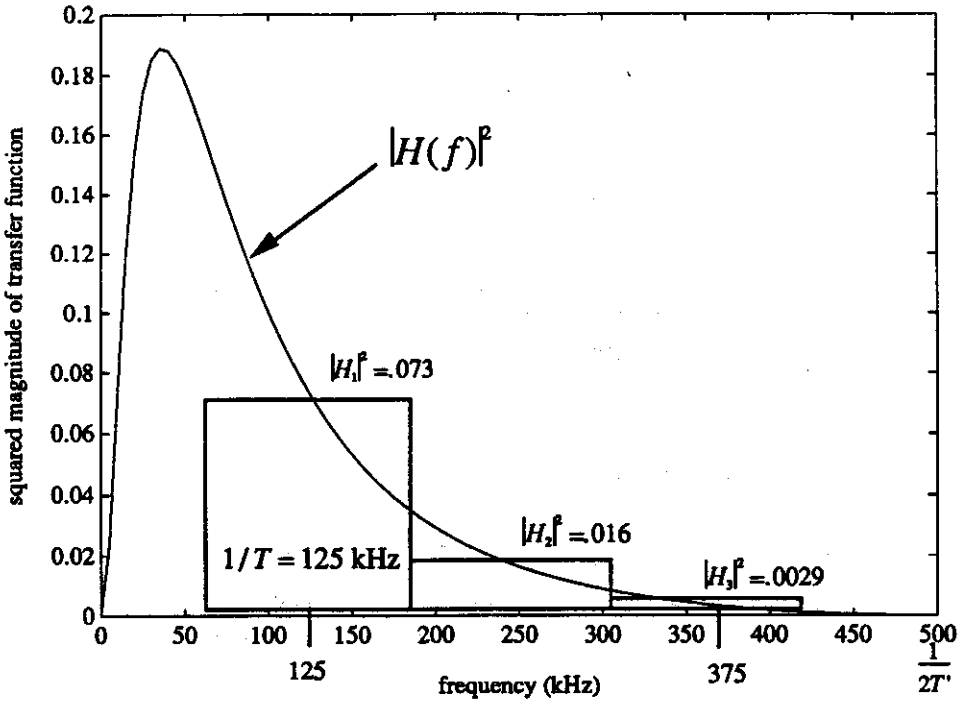

Figure 7: Example loop transfer function and the corresponding subchannel bands for $N = 8$ and $H(D) = \frac{.1(1-D^2)}{1-1.5D+.54D^2}$.

would proceed identically, but would required computer assistance for performance evaluation, see the appendix).

We have also illustrated the four corresponding subchannel frequency bands in Figure 7. The symbol rate is 1 MHz/8 = 125 kHz, so the center frequencies are

$$\begin{aligned} f_1 &= 125 \text{ kHz} \\ f_2 &= 250 \text{ kHz} \\ f_3 &= 375 \text{ kHz} \\ f_4 &= 500 \text{ kHz} \quad . \end{aligned}$$

One of the channels, $i = 4$, cannot be used because $H(0) = H(500 \text{ kHz}) = 0$. The other three subchannels have squared gains

$$\begin{aligned} |H_1|^2 &= .073 \\ |H_2|^2 &= .016 \\ |H_3|^2 &= .0029 \quad . \end{aligned}$$

We, thus, have a parallel independent set of subchannels with the above gains, each of which can be independently modulated and demodulated. We will return to this example again in Section 3 and analyze it in terms of achievable data rate at a given signal-to-noise ratio, or in terms of performance margin at an error rate of 10^{-7} and a given fixed data rate.

In this example, the portion of the channel characteristic with the greatest transfer magnitude (from 0 to 62.5 kHz in Figure 7) is ignored by this simple DMT system. However, by increasing N, the $\bar{N} - 1$ subchannel bands in Figure 7 become more narrow and cover an increasing fraction of the total

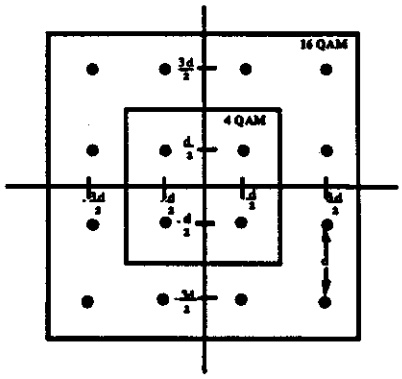

Figure 8: Square QAM constellations.

bandwidth. In the appendix, we cite results for this channel when DMT with $N = 512$ is used on this channel. The method for analysis will be the same in both the $N = 8$ and the $N = 512$ cases, it is just that the latter case will require the assistance of a computer to asses performance.

2 Single Carrier Analysis

Since multicarrier systems are equivalent to a set of independent (and also ISI-free) QAM subchannels, we can use single-carrier QAM analysis for a large part of the analysis of the multicarrier system. In this section, we describe a simple method for analyzing QAM, which is also described in a tutorial fashion in the upcoming overview by Forney and Eyuboglu of Codex in the December 1991 Communications Magazine [8]. A more complete paper by those two authors, and by the author of this report, on the analysis of single-carrier QAM systems appears in [9], which is available from this author on request.

2.1 The Square QAM approximation

Quadrature Amplitude Modulation (QAM) constellations may take a variety of forms, with perhaps the most well known constellations containing some power-of-4 points in two dimensions. When these points are arranged regularly within a square boundary, the constellation is said to be a QAM square. Square 4 QAM and 16 QAM constellations are illustrated in Figure 8, and 4 QAM, 64 QAM, 256 QAM, and even 1024 QAM are often encountered in data transmission applications. The distance between points in the contellation is denoted by d, and all points are assumed to be equally likely. The constellation is centered at the origin and has zero mean value. The energy of such a constellation is

$$\mathcal{E} = \frac{M-1}{6}d^2 \tag{6}$$

per two-dimensional symbol, where $M = 2^b$ is some power of 4 (b is an even integer) representing the number of points in the constellation, and b is the number of bits represented by a single QAM symbol. In practice, when $b \geq 2$ and odd or non-integer, then (6) is not exact, but still an accurate approximation to the transmit average energy. When $b < 2$, (6) is not a good approximation in general. However, with trellis coding, and in particular with the popular four-dimensional 16-state trellis code of Wei [10], it is possible for b to be as small as $b = 1/4$ and to use the relation in (6) without significant error. In so doing, $M = 2^b$ and is not necessarily the number of points in the two-dimensional QAM constellation when coded. Constellations with granularity to .5 bit (for example, $b = 3.5$) are readily

accomodated in the code case also. We thus will assume the relation in (6) is correct for any QAM constellation in the following method of analysis, but acknowledge that some cleverness[3] is required to make it strictly accurate for QAM channels with $b < 2$, as often arise in digital subscriber loop applications of multicarrier.

2.2 SNR Gap Analysis

We assume that the channel is ISI-free and has gain $|H|$. The probability of (two-dimensional) symbol error in QAM is closely approximated by

$$P_e \leq 4Q\left[\frac{d_{min}}{2\sigma}\right] \quad , \tag{7}$$

where d_{min} is the **minimum distance** between QAM constellation points at the channel output and is given by

$$d_{min}^2 = d^2|H|^2 \quad , \tag{8}$$

where $|H|$ is the channel gain and d is the distance between points in an uncoded input constellation. The well-known Q-function in (7) is defined by

$$Q[x] = \frac{1}{\sqrt{2\pi}}\int_x^\infty e^{-\frac{u^2}{2}}du \quad . \tag{9}$$

The probability of symbol error per dimension ($P_e/2$) should be 10^{-7} for DSL applications like HDSL and ADSL; to obtain this symbol error probability we require

$$\left(\frac{d_{min}}{2\sigma}\right)^2 = 14.5 \text{ dB} + \gamma_m \text{ dB} - \gamma_c \text{ dB} \quad . \tag{10}$$

The quantity γ_c is the **coding gain** of any applied code, including shaping gain/loss, nearest-neighbor penalties, and correlated-noise adjustments. The quantity γ_m is called the **margin**, an amount of extra performance that is required to ensure adequate performance in the presence of unforseen channel impairments. When γ_m and γ_c are zero, then the QAM system is uncoded and has no margin, and then we need 14.5 dB as an argument to the Q-function in (6) to get $P_e/2 = 10^{-7}$, a well-known result. When the system is coded, we reduce 14.5 dB by the amount of the coding gain, which is the amount by which d_{min} will appear to have been increased through the action of the code. When we desire a margin, we increase the 14.5 dB by the value of the margin. Typically, γ_m=6 dB for subscriber loop applications.[4] When we have both a margin and a code, we increase the 14.5 dB by the value of the margin less the gain of the code.

One can rewrite (6) in the form

$$M = 1 + \frac{6\mathcal{E}|H|^2}{d_{min}^2} \quad . \tag{11}$$

We define a convenient quantity called the **SNR gap**, Γ, (or sometimes the "normalized SNR") by

$$3 \cdot \Gamma = \frac{d_{min}^2}{4\sigma^2} \quad . \tag{12}$$

[3]More information of fractional bit constellations can be made available to Bellcore in the future, but a more detailed discussion is not necessary or appropriate in this document.

[4]Sometimes a margin of γ_m = 12 dB is requested for "theoretical" studies, implying that theory is likely to be incorrect by as much as an additional 6 dB with respect to lab measurements. This author's experience in using the theory in this document and comparing to actual measured system performance is that this theory is accurate to within 1 dB (and usually pessimistic), so we consistently maintain the use of a 6 dB margin in theoretical or lab analyses.

For our chosen target of $P_e/2 = 10^{-7}$, then we write that

$$(3 \cdot \Gamma)\ (\text{dB}) = 14.5 + \gamma_m - \gamma_c\ \text{dB} \quad . \tag{13}$$

By taking the log, base 2, of (11) and substituting (12) into (11) for d^2_{min}, one computes the number of bits that can be carried at $P_e/2 = 10^{-7}$ (with γ_m margin) by QAM:

$$b = \log_2(M) = \log_2\left(1 + \frac{SNR}{\Gamma}\right) \quad , \tag{14}$$

where SNR is the **channel output SNR** given by

$$SNR = \frac{\mathcal{E}|H|^2}{2\sigma^2} \quad . \tag{15}$$

The quantity Γ is called the "SNR gap" because we see in (14) that the number of bits that can be reliably transmitted is less than theoretical capacity ($C = \log_2[1 + SNR]$)for this channel and is the capacity of a channel with a factor of Γ less SNR. As Γ approaches 1 (0 dB), then the achievable data rate of the QAM system approaches capacity. The gap is then a measure of loss with respect to theoretically optimum performance. The gap is computed for any coded QAM system according to (13) as

$$\Gamma = 9.8 + \gamma_m - \gamma_c\ (\text{dB}) \quad , \tag{16}$$

where one need only know the margin desired in the system and the gain of any applied trellis code (when uncoded γ_c=0 dB). The SNR is also easily computed for any (ISI-free) QAM channel, so (14) gives a quick and easy method by which to compute accurately the number of bits per symbol, b, that can be achieved at $P_e/2 = 10^{-7}$ using QAM.[5] The data rate R can be computed from $R = b/T$, where T is the symbol period for the QAM system.

Often in practice, b is rounded to some integer value corresponding to some desired data rate R. In this case, we'd like to know the margin, γ_m that can be achieved at this fixed data rate with $P_e/2 = 10^{-7}$. To do this, we rewrite (14) as (using (16))

$$\Gamma = \frac{SNR}{2^b - 1} = 9.8 + \gamma_m - \gamma_c \quad . \tag{17}$$

Then

$$\gamma_m = 10\log_{10}\left(\frac{SNR}{2^b - 1}\right) + \gamma_c - 9.8\text{dB} \quad . \tag{18}$$

yields the margin for this data rate. The margin in (18) is often the quantity of interest in subscriber loop analysis.

2.3 Example

As an example of QAM analysis, let us examine a channel with $\mathcal{E} = 1$, $|H|^2 = 8$, and $\sigma^2 = .025$ with a symbol rate of $1/T = 400$ kHz. The SNR for this channel is computed to be $SNR = (1 \cdot 8)/(2 \cdot .025)$= 22 dB.

Let us first consider a case where there is no margin required ($\gamma_m = 0$ dB) and no code used ($\gamma_c = 0$ dB), then the gap is $\Gamma = 9.8$ dB. The data rate that can be achieved with $P_e/2 = 10^{-7}$ is computed according to (14) as

$$R = \frac{b}{T} = \frac{1}{T} \cdot \log_2\left(1 + \frac{10^{2.2}}{10^{.98}}\right) \approx 4 \cdot 400,000 = 1.6\ \text{Mbps} \quad . \tag{19}$$

[5]When using equalization with QAM on channels with intersymbol interference, SNR can be replaced with the SNR at the input to the decision element after the equalizer in (14) to compute the achievable data rate in the equalized case also.

The constellation used would be 16 QAM in this example.

Now, let us suppose we are forced to use a 6 dB margin so that $\gamma_m = 6$ dB; then, the gap increases to 15.8 dB. Recomputing the data rate with this margin produces

$$R = \frac{b}{T} = \frac{1}{T} \cdot \log_2\left(1 + \frac{10^{2.2}}{10^{1.58}}\right) \approx 2 \cdot 400,000 = 800 \text{ kbps} \quad . \tag{20}$$

The constellation used would now be 4 QAM.

Let us now assume that we desire 1.8 Mbps on this channel and use a powerful trellis code with $\gamma_c = 5.0$ dB. Then $b = 4.5$ bits/symbol. Then the margin is computed according to (18) as

$$\gamma_m = 10 \cdot \log_{10}\left(\frac{10^{2.2}}{2^{4.5} - 1}\right) + 5.0 - 9.8 \text{ dB} \approx 3.9 \text{ dB} \quad . \tag{21}$$

For channels with intersymbol inteference and equalization, one can replace the SNR in the above examples by the SNR at the detection element input in the receiver and the analysis will remain very accurate.

3 Analysis of Discrete Multitone

Having established the QAM single-carrier analysis in Section 2, we now use it to analyze multicarrier as an aggregate of ISI-free QAM subchannels.

3.1 Designing for the Weak-link

The probability of error for a multicarrier system is the average of the probabilities of error for each of the subchannels. In such an average, those subchannels with largest probabilities of error would dominate. Then, in well-designed multicarrier systems, we choose the same probability of error for all subchannels so that no one subchannel is any better than the others.[6]

We choose our probability of subsymbol error to be equal on all subchannels and, again, at the level of $P_e/2 = 10^{-7}$. Then the analysis of Section 2 directly applies to each subchannel. We have a constant gap, Γ, on all subchannels, again computed according to (16). We now write for the i^{th} subchannel that

$$3\Gamma = \frac{d^2_{min,i}}{4\sigma_i^2} = \frac{|H_i|^2 d_i^2}{4\sigma_i^2} \tag{22}$$

where the subscript of i is added to all quantities that can vary from subchannel to subchannel. Again for any subchannel, the analysis of Section 2 directly applies, and so we may write

$$b_i = \log_2\left(1 + \frac{SNR_i}{\Gamma}\right) \tag{23}$$

as the maximum number of bits per symbol that can be carried on that subchannel with margin γ_m and coding gain γ_c. The quantity SNR_i is computed by

$$SNR_i = \frac{|H_i|^2 \mathcal{E}_i}{2\sigma_i^2} \tag{24}$$

[6]It has been noted that multicarrier provides an easy way to have more critical information assigned to those subchannels for which the design ensures a lower probability of error than on other subchannels. Such channels might carry control information or critical components of a compressed video signal. While Amati intends to take advantage of this strong point of multicarrier in products, we leave further study of this option to future discussions of applications of ADSL where this unequal error protection may be desirable.

where we always choose $\mathcal{E}_i = \mathcal{E}$ constant on those subchannels that are used and zero on subchannels not used. (There is actually a better energy distribution called the "water-pouring" distribution, see [1], but we have found that the on/off energy distribution is very close to this optimum on all channels we have analyzed and the on/off is easier to compute.) We assume constant gain and margin on all subchannels because we desire the same probability of error on each subchannel, which is what forces Γ to be constant (independent of i) above.

3.2 Computing Rate or Margin

The total number of bits that is transported in one symbol is then the sum of the number of bits on each of the subchannels, so

$$b = \sum_{i=1}^{\tilde{N}} b_i = \sum_{i=1}^{\tilde{N}} \log_2 \left(1 + \frac{SNR_i}{\Gamma}\right) \quad . \tag{25}$$

Then the data rate is $R = b/T$.

An alternative relationship to (25) is

$$b = \log_2 \left[\prod_{i=1}^{\tilde{N}} \left(1 + \frac{SNR_i}{\Gamma}\right)\right] \quad . \tag{26}$$

By defining an "average SNR", $\overline{SNR}$, by

$$1 + \frac{\overline{SNR}}{\Gamma} = \left[\prod_{i=1}^{\tilde{N}} \left(1 + \frac{SNR_i}{\Gamma}\right)\right]^{1/\tilde{N}} \quad , \tag{27}$$

or

$$\overline{SNR} = \Gamma \left\{ \left[\prod_{i=1}^{\tilde{N}} \left(1 + \frac{SNR_i}{\Gamma}\right)\right]^{1/\tilde{N}} - 1 \right\} \quad , \tag{28}$$

we can rewrite (25) more simply as

$$b = \tilde{N} \cdot \log_2 \left(1 + \frac{\overline{SNR}}{\Gamma}\right) \quad . \tag{29}$$

From the form of (29) we see that $\overline{SNR}$ can be directly compared against the detection SNR for a single-carrier QAM system at the same number of bits per symbol ($b_{QAM} = b_{DMT}/\tilde{N}$). The form of the relation in (29) also permits direct computation of a margin for a multicarrier system with fixed data rate and probability of error. To do so, we note that the "1+" and "-1" terms in (27) are often negligible and may be ignored to a first order approximation so that our average SNR becomes the geometric average

$$\overline{SNR} \approx \left[\prod_{i=1}^{\tilde{N}} (SNR_i)\right]^{1/\tilde{N}} \quad , \tag{30}$$

which does not involve the gap (which is unknown if we are trying to compute the margin). One must take care in dropping the "1+" and "-1" terms to alter $\tilde{N}$ to the number of used subchannels (that is, do not count channels with zero input energy) in computing the margin. Then, we may compute the margin by rewriting (29) as

$$\gamma_m = 10 \log_{10} \left(\frac{\overline{SNR}}{2^{b/\tilde{N}} - 1}\right) + \gamma_c - 9.8\text{dB} \quad . \tag{31}$$

In (31), $\bar{N}$ is again the number of used subchannels. At a fixed data rate R, $b = RT$, and (31) can be used to compare against a single-carrier system with the same target P_e.

3.3 Example

Returning to the example of Section 1, let us use $\mathcal{E} = 1$ for $i = 1, 2, 3$. Further let us assume a crosstalking noise that increases in power with frequency as $f^{1.5}$ appears on this channel. The corresponding subchannel noise variances are $\sigma_1^2 = 10^{-5}/2$, $\sigma_2^2 = 2.82 \times 10^{-5}/2$, and $\sigma_3^2 = 5.2 \times 10^{-5}/2$. Then the subchannel signal to noise ratios, computed according to (24) are

$$\begin{aligned} SNR_1 &= \frac{1 \cdot .073}{10^{-5}} = 7300 \ (38.6 \text{ dB}) \\ SNR_2 &= \frac{1 \cdot .016}{2.82 \times 10^{-5}} = 567 \ (27.5 \text{ dB}) \\ SNR_3 &= \frac{1 \cdot .0029}{5.2 \times 10^{-5}} = 56 \ (17.4 \text{ dB}) \quad . \end{aligned}$$

With no margin and no code, the achievable data rate is

$$\begin{aligned} R = \frac{b}{T} &= 125 \text{ kHz} \cdot \left\{ \log_2 \left(1 + \frac{7300}{10^{.98}} \right) + \log_2 \left(1 + \frac{567}{10^{.98}} \right) + \log_2 \left(1 + \frac{56}{10^{.98}} \right) \right\} \\ &= 18.2 \cdot 125 \text{ kHz} = 2.3 \text{ Mbps} \quad . \end{aligned} \tag{32}$$

With a powerful trellis code of gain 5 dB, we would like to know the margin at 1.75 Mbps. First, we compute the geometric average SNR for the three channels as

$$\overline{SNR} = [7300 \cdot 567 \cdot 56]^{1/3} = 614 \quad . \tag{33}$$

(Note, we have used the number of used subchannels, $\bar{N} = 3$.) The number of bits per symbol required to achieve 1.75 Mbps is 14. Then, we compute the margin from (31) to get

$$\gamma_m = 10 \cdot \log_{10}\left(\frac{614}{2^{14/3} - 1}\right) + 5.0 - 9.8 \text{ (dB)} = 9.2 \text{ dB} \quad . \tag{34}$$

With this small of an FFT size, the subchannels are not really independent, so only the method of analysis is illustrated with this example. Nevertheless, if N is increased to 512, the reader will find that this analysis will accurately project the achievable data rate or margin for DMT on subscriber loops. The methods in the appendix simply ensure that the analysis for block-length $N = 512$ is accurate by forcing the 256 derived subchannels to be independent, and thus altering the H_i slightly from $H(f_i)$.

3.4 Review of Performance Calculation

The procedure to analyze the multicarrier system can by summarized in the following four steps:

1. From the power budget, compute a preliminary subsymbol energy allocation according to $\mathcal{E} = \mathcal{E}_i = (PT)/\bar{N}$.

2. Compute the subchannel SNR's according to

$$SNR_i = \frac{\mathcal{E}|H_i|^2}{\sigma_i^2} \quad . \tag{35}$$

3. Compute the number of bits that can be transmitted on each subchannel with a given margin and given trellis code (thus determining $\Gamma = 9.8 + \gamma_M - \gamma_c$ dB) as

$$b_i = \log_2\left(1 + \frac{SNR_i}{\Gamma}\right) \quad . \tag{36}$$

4. For those subchannels with $b_i < .5$, reset $\mathcal{E}_i = 0$ and reallocate their energy to the other subchannels equally. Then, recompute b_i.

5. Compute b by summing the b_i, and then compute the maximum data rate $R = b/T$.

A margin can be computed using any number of used subchannels. For data rates considerably below theoretical optimums, the number of used subchannels often decreases with respect to the bandwidth used for the maximum data rate. The geometric average $\overline{SNR}$ in (30) can be computed recursively by ordering the $|H_i|^2/\sigma_i^2$ and incorporating the largest SNR_i first, then the next largest, etc. Each of these $\overline{SNR}_i$ can in turn be used in (31) to compute a margin. The bandwidth with the best margin is then used for this target (lower than maximum) data rate.

A DMT with finite block length

Strictly speaking, the subchannels discussed in Sections 1 and 3 are not independent for finite N. Nevertheless, it is possible to make them exactly independent (white Gaussian noise case) by using what is known as a cyclic prefix [2]. The Discrete Fourier Transform (DFT) of a time-domain sequence is defined by (dropping the block symbol index k from all subscripts)

$$X_i = \frac{1}{\sqrt{N}} \sum_{n=0}^{N-1} x_n e^{-\jmath \frac{2\pi}{N} in} \quad , \tag{37}$$

where $\jmath \triangleq \sqrt{-1}$. The Fast Fourier Transform (FFT) is a computationally efficient method for computing the DFT when N is some convenient number, usually a power of 2. We use the term "FFT" synonymously with "DFT," even though it is somewhat of a misnomer. The inverse FFT (or IFFT) is given by

$$x_n = \frac{1}{\sqrt{N}} \sum_{i=0}^{N-1} X_i e^{\jmath \frac{2\pi}{N} in} \quad , \tag{38}$$

where, given X_i, $i = 1, ..., \bar{N}$ as in the body of this document, X_i in (38) is found as

$$X_i = \begin{cases} X_i & i = 1, ..., \bar{N} - 1 \\ \Re(X_{\bar{N}}) & i = 0 \\ \Im(X_{\bar{N}}) & i = \bar{N} \\ X^*_{N-i} & i = \bar{N} + 1, ..., N - 1 \end{cases} \quad . \tag{39}$$

The conjugate symmetry conditions on X_i are imposed to force x_n to be a real sequence. Likewise, when x_n is real, these conditions will hold.

In continuous time, a well-known result is that convolution in the time domain corresponds to multiplication of Fourier Transforms. In discrete time this result only holds if one of two conditions is met: (1) the block length N is infinite or (2) at least one of the input sequences convolved is periodic with period N. That is, we may write

$$x_n * h_n \Longleftrightarrow X_i \cdot H_i \quad , \tag{40}$$

if either of the above conditions is met. Otherwise, multiplication in the frequency domain does not correspond to time-domain convolution.

In practice, N is never infinite, so we would like to make it appear as if x_n were periodic. We assume that h_n is limited to being nonzero only over the time index range $0 \leq n \leq \nu$, where ν is sometimes called the **constraint length** of the channel. For any practical channel, we can always approximate this finite-length condition by just picking ν sufficiently large. We note that if we prefix a time-domain block of samples x_n, $n = 0, ..., N-1$ by the last ν samples of that block, we get a new block of length $N+\nu$, indexed from $n = -\nu, ..., 0, ..., N-1$. For the N samples of the convolution $y_n = h_n * x_n$, $n = 0, ..., N-1$, we note that

$$y_n = \sum_{k=0}^{\nu} h_k x_{n-k} \tag{41}$$

depends only on x_n within our prefixed block. Furthermore, for these values of y_n only, it appears as if x_n were indeed periodic over all time. Thus, by using the cyclic prefix, we ensure that the relation

$$Y_i = H_i X_i \quad i = 1, ..., \bar{N} \tag{42}$$

(where $H_{\bar{N}}$ is understood to be $H_{\bar{N}} = H_0 + \jmath\Im(H_{\bar{N}})$) holds exactly. Of course, ν samples are wasted with the prefix, thus decreasing the data rate R by a factor of $N/(N+\nu)$. If $N >> \nu$, then this loss is negligible.

Cyclic prefix is used in most good multicarrier designs, see [11] and [5] for those in commercial products. Unfortunately, in subscriber loops, ν can be very large, perhaps hundreds of sample periods at practical sampling rates. Then N would need to be enormous for the rate loss, $N/(N+\nu)$, to be negligible. Fortunately, J.S. Chow has derived a novel method by which to reduce the value of $\bar{N}$ required substantially without reducing performance [6]. We model the channel polynomial, defined as

$$H(D) = \sum_n h_n D^n \quad , \tag{43}$$

as a rational polynomial

$$H(D) = \frac{B(D)}{A(D)} \quad , \tag{44}$$

where $B(D)$ is a zero polynomial, $B(D) = \sum_{n=n'}^{n'+\nu} b_n D^n$ of order ν and $A(D)$ is a monic ($a_0 = 1$), causal ($a_n = 0, n < 0$) pole polynomial of order μ, $A(D) = 1 + \sum_{n=1}^{\mu} a_n D^n$. For subscriber loops, we rarely need ν or μ greater than 10 to model the channel accurately, even at very high sampling rates. A first method to reduce the channel would be to filter the channel with $A(D)$, which would leave an "equalized" channel of $B(D)$. Then, a much shorter FFT size could be used on this equalized channel, because $\nu < 10$. However, the SNR_i are severely degraded when such an approach is taken.

We prefer to find an equalizer $\tilde{A}(D)$, used as shown in Figure 9, of μ taps (or less) and a target polynomial $\tilde{B}(D)$ such that the SNR

$$SNR = \frac{\mathcal{E}\|\tilde{B}(D)\|^2}{\|\tilde{A}(D)Y(D) - \tilde{B}(D)X(D)\|^2} \tag{45}$$

is maximized, where $\|\tilde{B}(D)\|^2 = \sum_{n=n'}^{n'+\nu} \tilde{b}_n^2$ and likewise for the norm of the denominator in (45). We also note that $\tilde{B}(D)$ need not be causal, and indeed is usually not. A good (but perhaps not absolute best) solution to this problem can be derived from what is known as an ARMA (autoregressive moving average) model for the channel [12]. This problem is more general than decision feedback equalization (which imposes an additional restriction that $B(D)$ be causal so that trailing ISI can be cancelled), and the SNR

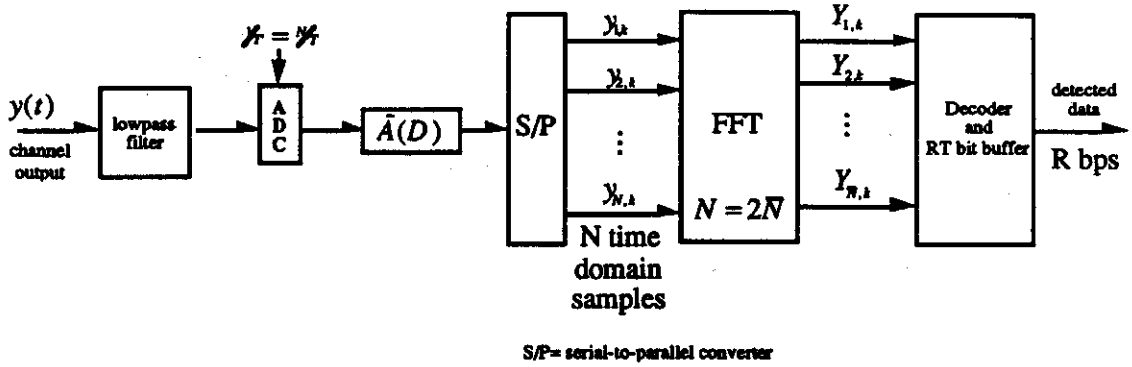

Figure 9: Chow's DMT receiver with short equalizer $\tilde{A}(D)$. The equalzer is used to decrease the apparent channel response length while simultaneously preserving good SNR in the resultant controlled intersymbol-interference channel. The S/P is also presumed to ignore all ν samples per symbol that are influenced by the previous block with cyclic prefixing.

in (45) is greater than that of a decision feedback equalizer applied to the same channel. With μ greater than or equal to the maximum number of poles in channel models, we have found this ARMA equalizer method to achieve near infinite-length multicarrier performance as long as $N >> \nu$. For subscriber loops with $\nu < 20$, $N = 512$ ($\bar{N} = 256$) achieves near optimum performance. The noise variances at each frequency, σ_i^2, are computed by forming the power spectral density of $\tilde{A}(D)Y(D) - \tilde{B}(D)X(D)$ and sampling at the proper frequencies. The channel gains H_i are replaced by the gains $\tilde{B}_i \triangleq \tilde{B}(e^{j2\pi f_i T})$. The i^{th} subchannel SNR is then $SNR_i = \frac{\mathcal{E}|\tilde{B}_i|^2}{\sigma_i^2}$.

The ARMA model for a channel can be found with a number of software packages for analysis, or the author can provide a method to compute the ARMA model easily upon request. In actual implementation, the ARMA model can be found by using an adaptive (i.e., LMS gradient) algorithm on the adaptive filter shown in Figure 10 when the input sequence (training) is known to the receiver.

A.1 Example

We now return to the example of Sections 1 and 3 one last time. We assume an additive white Gaussian noise with variance per dimension $\sigma^2 = 4 \times 10^{-5}$. Using an ARMA 3-tap equalization filter of $\tilde{A}(D) = 1 - 1.459D + .517D^2$, then $\tilde{B}(D) = .1 + .0043D - .0961D^2$ and the noise at the equalizer output is correlated according to the shaping of $\tilde{A}(D)$, but nevertheless independent from frequency to frequency when we use $N = 512$. This equalized system with the resulting $\bar{N} = 256$ (maximum) subchannels will achieve a data rate of 2.3 Mbps with no margin and no code. Using the same block length and ignoring the equalization and cyclic prefix (and just using the H_i for the original channel characteristic directly), we would have computed 2.5 Mbps. That latter analysis is slightly optimistic because the channels are not quite independent unless the equalization method of this appendix is used, which reduces the actual performance slightly. With γ_m= 6 dB, the ARMA-equalizer method yields 1.6 Mbps (while ignoring equalization produces 1.7 Mbps). Various bias-removal methods can be used to increase 2.3 Mbps to

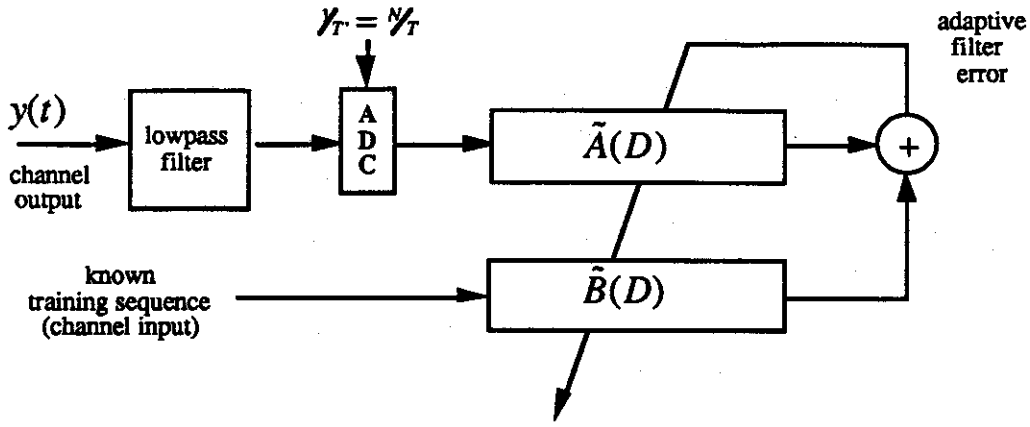

Figure 10: Illustration of adaptive filter necessary to obtain ARMA channel model. The filter $\tilde{A}$ is used for "equalizing" the sampled channel output prior to the FFT in the DMT receiver after training with this configuration. The reader is cautioned not to assume that this configuration is a decision feedback equalizer; it is not. The polynomial $\tilde{B}(D)$ is not necessarily minimum-phase nor causal and $\tilde{A}(D)$ and $\tilde{B}(D)$ are much shorter than the feedforward and feedback sections of a DFE for the same channel.

2.5 Mbps and 1.6 Mbps to 1.7 Mbps so that the straightforward analysis results can be achieved in an implementable system.

Finally, with $\gamma_c = 5$ dB and a target data rate of 1.8 Mbps, the margin is 9.7 dB. The reader will need a computer to verify the numbers in this last section, but analysis proceeds exactly as illustrated earlier, just with a larger number of subchannels.

References

[1] R.G. Gallager. *"Information Theory and Reliable Communication"*. Wiley, New York, NY, 1968.

[2] A. Peled and A. Ruiz. "Frequency Domain Data Transmission using Reduced Computational Complexity Algorithms". In *International Conference on Acoustics, Speech, and Signal Processing*, April 1980. Denver, pp. 964-967.

[3] A. Ruiz, J.M. Cioffi, and S. Kasturia. "Discrete Multiple Tone Modulation with Coset Coding for the Spectrally Shaped Channel". *IEEE Transactions on Communications*, to appear 1991.

[4] A. Ruiz and J.M. Cioffi. "A Frequency-Domain Approach to Combined Spectral Shaping and Coding". In *ICC'87*, pages 1711–1715, Seattle, WA, June 1987.

[5] J.M. Wozencraft and P.H. Moose. "Modulation and Coding for In-Band Digital Audio Broadcast using Multi-Frequency Modulation". In *National Association of Broadcasters 1991 Conference Proceedings, see also Radio 1991 Proceedings (San Francisco, 9/91)*, Las Vegas, April 1991.

[6] J.S. Chow, J. Tu, and J.M. Cioffi. "A Discrete Multitone Transceiver System for HDSL Applications". *IEEE Journal on Selected Areas in Communication*, 8(4):??, August 1991.

[7] P.S. Chow, J. Tu, and J.M. Cioffi. "Performance Evaluation of a Multichannel Transceiver System for ADSL and VHDSL Services". *IEEE Journal on Selected Areas in Communication*, 8(4):??, August 1991.

[8] G.D. Forney Jr. and M.V. Eyuboglu. "Combined Equalization and Coding using Precoding". *IEEE Communications Magazine*, 29(12), December 1991.

[9] J.M. Cioffi, G.P. Dudevoir, M. V. Eyuboglu, and G.D. Forney. "MMSE Decision-Feedback Equalizers and Coding – Part I: General Results". submitted, IEEE transactions on Communications, 5/90.

[10] G.D. Forney Jr. "Coset Codes - Part I: Introduction and Geometrical Classification". *IEEE Transactions on Information Theory*, 34(5):1123–1151, September 1988.

[11] J.A.C. Bingham. "Multicarrier Modulation for Data Transmission: An Idea Whose Time has Come". *IEEE Communications Magazine*, 28(4):5–14, April 1990.

[12] S. Haykin. *Adaptive Filter Theory*. Prentice-Hall, Englewood Cliffs, NJ, 1985.